© 2021. Published by The Company of Biologists Ltd | Journal of Cell Science (2021) 134, jcs256818. doi:10.1242/jcs.256818

RESEARCH ARTICLE

Nucleoporin 50 mediates *Kcna4* transcription to regulate cardiac electrical activity

Xueting Gao[1,2,3,*], Shuai Yu[1,2,3,*], Yi Guan[1,2,3], Yunli Shen[1,2,‡] and Liang Xu[1,2,3,‡]

ABSTRACT

Emerging evidence has demonstrated that nucleoporins (Nups) play a pivotal role in cell-type-specific gene regulation, but how they control the expression and activity of ion channel genes in the heart remains unclear. Here, we show that Nup50, which is localized in the nucleus of cardiomyocytes, selectively induces an increase in the transcription and translation of *Kcna4*. The *Kcna4* gene encodes a K^+ voltage-gated channel of shaker-related subfamily member 4 and is essential for regulating the action potential in cardiac membranes. Using immunofluorescence imaging, luciferase assays and chromatin immunoprecipitation assays, we identified that the direct binding of the FG-repeat domain within Nup50 to the proximity of the *Kcna4* promoter was required to activate the transcription and subsequent translation of *Kcna4*. Functionally, Nup50 overexpression increased the currents of *KCNA4*-encoded $I_{to,s}$ channels, and reverse knockdown of Nup50 resulted in a remarkable decrease in the amplitude of $I_{to,s}$ currents in cardiomyocytes. Moreover, a positive correlation between Nup50 and *Kcna4* mRNA and protein expression was observed in heart tissues subjected to ischemic insults. These findings provide insights into the homeostatic control of cardiac electrophysiology through Nup-mediated regulation.

KEY WORDS: Nucleoporins, Transcriptional regulation, Ischemic, Cardiac electrical activity

INTRODUCTION

The nuclear pore complex (NPC) represents a supramolecular complex that resides in the double membrane surrounding the eukaryotic cell nucleus. In mammalian cells, NPCs comprise ∼30 different proteins termed nucleoporins (Nups). There is an eightfold-symmetrical structure in the NPC, which builds a nuclear envelope-embedded scaffold enclosing a central transport channel. The nuclear and cytoplasmic filaments of NPCs are flexible fibrils, and the nuclear filaments are connected to a distal ring, forming a structure called the nuclear basket (Beck and Hurt, 2017). Owing to its envelope localization, NPCs have long been considered to function as portals that control the transport of protein and RNA between the nucleus and cytoplasm. However, several studies have identified roles for individual nucleoporins in transcriptional activation, elongation, RNA processing, RNA stabilization, gene silencing and heterochromatin formation, indicating that nucleoporins fulfill diverse functions in gene regulation and chromatin biology (Knockenhauer and Schwartz, 2016). Moreover, tissue-specific expression of nucleoporins and cell cycle-adjusted changes in nucleoporin abundance can add another layer of complexity to NPC function (Raices and D'Angelo, 2012).

An anomaly of Nups is that they are associated with many human diseases, including immune diseases, neurological diseases, cancer and cardiovascular disorders (Nofrini et al., 2016). A close link between Nup abnormality and cardiovascular disease was first reported in a family with atrial fibrillation segregating with a Nup155 homozygous variant (Zhang et al., 2008). The upregulated expression levels of Nup160 and Nup153 have been found to be involved in cardiac tissues of patients with heart failure (Tarazón et al., 2012). In our previous study, we reported that Nup35 posttranscriptionally regulated cardiomyocyte pH homeostasis by controlling Na^+-H^+ exchanger-1 (Nhe1) expression and that the mRNA level of Nup50 was dramatically increased in a model of hypoxia and acute myocardial infarction (Xu et al., 2015).

Nup50 is a mobile nucleoporin that localizes in the nuclear basket, via its interaction with Nup153 (Makise et al., 2012), and in the nucleoplasm (Guan et al., 2000). Nup50 regulates nuclear transport of protein and RNA (Moore, 2003; Matsuura and Stewart, 2005). Two human Nup50 isoforms, the long (Nup50L) and short (Nup50S) forms, differentially regulate nuclear protein import (Ogawa et al., 2010). A recent study demonstrated that Nup50 exhibits transcription-dependent profiles both at the NPC and within the nucleoplasm, and this feature required ongoing RNA Pol II association with chromatin and was independent of importin-α, Nup153 and Nup98 (Buchwalter et al., 2014), indicating a transport-independent role of Nup50 in chromatin biology that extended from the NPC.

In the present study, we demonstrated that Nup50 transcriptionally regulates the expression of the *Kcna4* gene in cardiomyocytes. The FG-repeat domain was responsible for the interaction of Nup50 with the proximal promoter of the *Kcna4* gene. The overexpression of Nup50 significantly increased the *Kcna4*-encoded slowly inactivating transient outward K^+ channel ($I_{to,s}$) current.

RESULTS

Nup50 selectively regulates the expression of *Kcna4*-encoded K^+ channels in cardiomyocytes

Many of the deaths after myocardial ischemia or infarction are attributed to the development of cardiac arrhythmias. Myocardial ischemia is characterized by ionic and metabolic alterations, creating an unstable electrical substrate capable of initiating and sustaining arrhythmias. Our previous study showed that Nup50 was the most elevated nucleoporin among the nuclear pore complexes in

[1]Department of Cardiology, East Hospital, Tongji University School of Medicine, Shanghai 200120, China. [2]Key Laboratory of Arrhythmias of the Ministry of Education of China, Tongji University School of Medicine, Shanghai 200120, China. [3]Institute of Medical Genetics, Tongji University, Shanghai 200092, China.
*These authors contributed equally to this work

‡Authors for correspondence (shenyunli2011@163.com; xuliang_east@126.com)

Y.S., 0000-0002-3204-6594; L.X., 0000-0002-1479-2163

Handling Editor: Maria Carmo-Fonseca
Received 8 November 2020; Accepted 12 August 2021

Journal of Cell Science (2021) 134, jcs256818. doi:10.1242/jcs.256818

a model of hypoxia and acute myocardial infarction (Xu et al., 2015). To explore whether Nup50 regulates the expression of ion channels, we changed the expression of Nup50 to measure its effect on the mRNA levels of major ion channels expressed in neonatal rat ventricular myocytes (NRVMs). The knockdown efficiency was evaluated with a quantitative PCR (qPCR), and the effective siRNA sequence was adopted for the knockdown experiment (Fig. S1A,B). As shown in Fig. 1A, the reduction in Nup50 protein downregulated the mRNA expression of *Kcna4* but did not affect other ion channels, such as *Scn5a*, *Cacna1c*, *Kcnd2*, *Kcnd3* and *Kcnj2*. Conversely, the overexpression of Nup50 selectively increased the expression of *Kcna4* mRNA (Fig. 1B; Fig. S1C). As a sole reference gene may cause problematic qualification (Ling and Salvaterra, 2011), other internal references, β-actin and 18 s, were also chosen to determine the effects of Nup50 on *Kcna4* mRNA levels. Our data demonstrated that Nup50 regulated the expression of *Kcna4* mRNA (Fig. 1C,D).

We further studied the effects of Nup50 on the protein expression of the *Kcna4*-encoded Kv1.4 channel in NRVMs. Our data showed that Nup50 depletion decreased the expression of Kv1.4 proteins (Fig. 1E; Fig. S1D), whereas knockdown of Nup153 had no such effect (Fig. 1F). Conversely, ectopic overexpression of Nup50 increased the protein expression of Kv1.4 (Fig. 1G; Fig. S1E). These results were consistent with the effects of Nup50 on *Kcna4* mRNA in NRVMs. In addition, Myc-tagged Nup50 was utilized to confirm the activation function of GFP-tagged Nup50 when introduced into NRVMs (Fig. S1F–H). These results demonstrate that Nup50 modulates the expression of cardiac *Kcna4* at both the mRNA and protein levels.

Nup50 promotes *Kcna4* transcription by targeting its proximal promoter

Next, we asked whether the Nup50-mediated modulation of the expression of *Kcna4*-encoded proteins occurred at the transcription

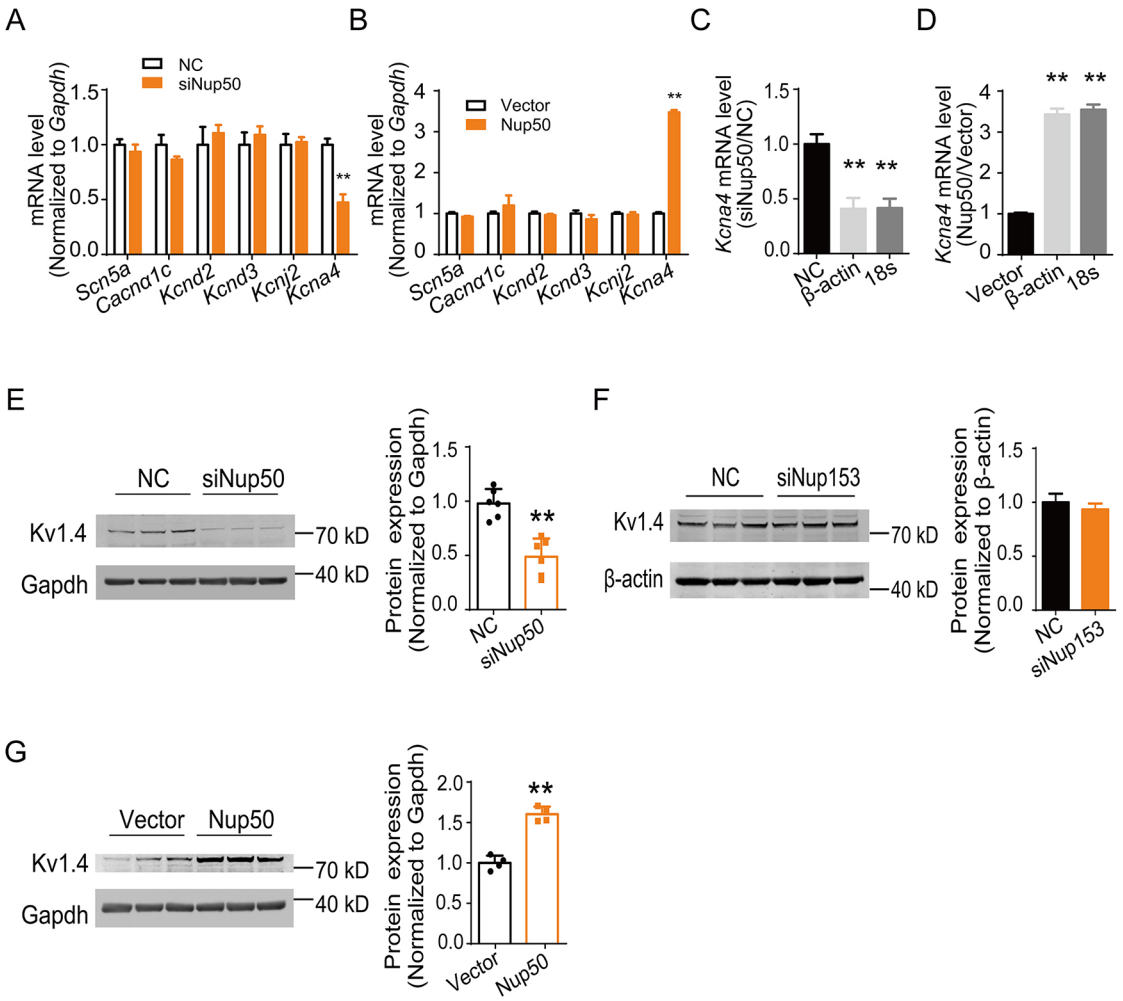

Fig. 1. Nup50 affects the expression of *Kcna4* in NRVMs. qPCR analysis of the effects of Nup50 knockdown on a Na^+ channel (*Scn5a*), a Ca^{2+} channel (*Cacna1c*) and K^+ channels (*Kcnd2*, *Kcnd3*, *Kcnj2* and *Kcna4*). NRVMs were treated with either scramble RNA (negative control, NC) or Nup50 siRNA for 48 h, followed by the detection of the expression of the main ion channels on NRVMs. Data were pooled from three independent experiments. (B) The mRNA levels of the main ion channels 48 h after Nup50 overexpression. NRVMs were treated with either control vector (harboring GFP) or Nup50–GFP for 48 h, followed by the detection of the expression of the Na^+, Ca^{2+} and K^+ channels. The mRNA level of *Kcna4* in Nup50-depleted (C) or Nup50-overexpressing (D) NRVMs is shown. Data were normalized to β-actin and 18 s and pooled from three independent experiments. Western blotting analysis of the impact of Nup50 knockdown (siNup50) (E) or Nup153 knockdown (siNup153) (F) on Kv1.4 protein expression in NRVMs. NRVMs were treated with either Nup50 siRNA or Nup153 siRNA for 48 h, followed by the detection of the expression of Kv1.4. (G) Western blotting analysis of the impact of Nup50 overexpression on Kv1.4 protein expression in NRVMs. NRVMs were treated with either control vector expressing GFP or Nup50-overexpressing vector Nup50-GFP for 48 h, followed by the detection of the expression of Kv1.4. Results in E–G are for at least three experiments. Data shown are mean±s.d. $^{**}P<0.01$ (unpaired, two-tailed *t*-test for two-group comparisons and one-way ANOVA followed by Tukey's post hoc test for multiple-group comparisons).

Journal of Cell Science (2021) 134, jcs256818. doi:10.1242/jcs.256818

stage. Using either primers that annealed to the introns of the *Kcna4* mRNA precursor or primers for the exons, which detect the mature spliced *Kcna4* mRNA, we analyzed *Kcna4* expression levels in Nup50-overexpressing or Nup50-depleted NRVMs (Fig. 2A). Compared with the control vector harboring GFP, Nup50 overexpression dramatically increased the production of nascent and mature *Kcna4* mRNAs (Fig. 2B), and conversely, the ablation of Nup50 led to their decrease (Fig. 2C).

To confirm the active effects of Nup50 on *Kcna4* transcription, we cloned the *Kcna4* promoter from rat genomic DNA and inserted it into the 5′ position of the luciferase gene to substitute for the original SV40 early enhancer/promoter of the psiCHECK-2 vector (Fig. 2D). The effective promoter region was identified as the proximal 1000 nt upstream of the transcription beginning site of the *Kcna4* gene (Fig. 2E). Next, the dual-luciferase reporter containing the effective *Kcna4* promoter was co-transfected with GFP or Nup50 and the relative luminescence intensity in NRVMs was compared. Our results showed that, compared to the GFP group, the ectopic expression of Nup50 was sufficient to increase the luminescence value in cardiomyocytes (Fig. 2F), whereas the knockdown of Nup50 significantly decreased the luminescence activity (Fig. 2G). These results suggested that the Nup50-mediated regulation of *Kcna4* expression was involved in direct targeting to the proximal region of the *Kcna4* promoter.

Nup50 directly binds to the promoter of *Kcna4* in cardiac myocytes

To further investigate how Nup50 interacted with the *Kcna4* promoter, the localization of Nup50 was examined. As shown in Fig. 3A, GFP-tagged Nup50 was distributed in the nucleoplasm in a punctuate pattern, which was the same as seen for endogenous Nup50 recognized by the specific antibody (Fig. S2A). Nup50 was broadly distributed through the nucleoplasm and excluded from regions of highly condensed chromatin (Fig. S2B–D). This close spatial

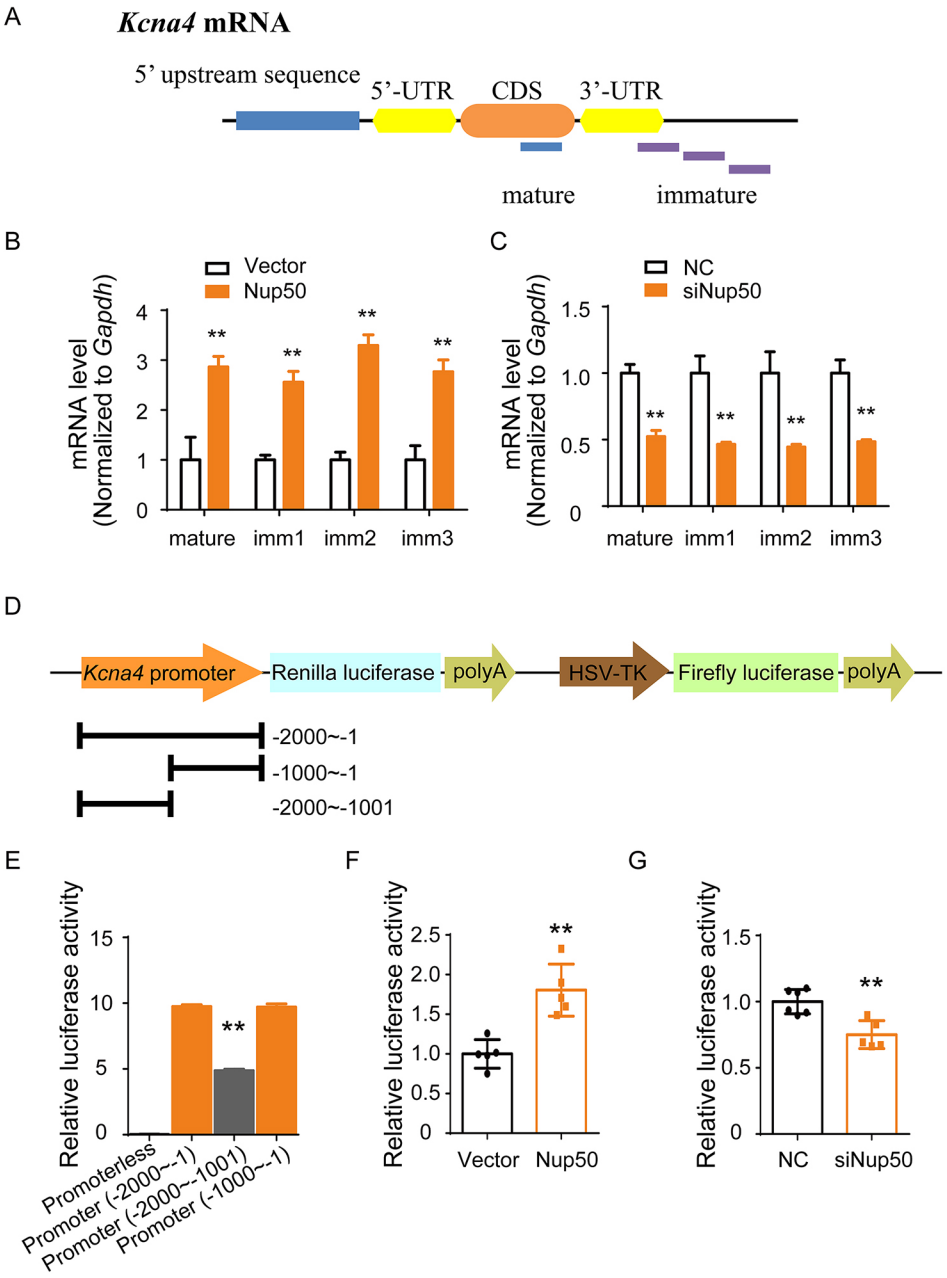

Fig. 2. Nup50 regulates *Kcna4* expression by targeting its promoter. (A) Schematic diagram of amplification regions of nascent and mature (blue) *Kcna4* mRNA. Immature (imm1–imm3); purple. The effects of Nup50 overexpression (B) and knockdown (siNup50) (C) on the expression of *Kcna4* mRNA. Data are presented as the expression of *Kcna4* mRNA relative to the internal reference *Gapdh*. Data were pooled from three independent experiments. (D) Schematic diagram of the luciferase reporter vector containing the *Kcna4* promoter. (E) The luminescence intensity of the truncated *Kcna4* promoter. NRVMs were treated with different *Kcna4* promoter truncates for 48 h, followed by the detection of luciferase activity. (F) The luminescence intensity of the *Kcna4* promoter in Nup50-overexpressing cardiomyocytes. NRVMs were transfected with either control vector (GFP) or Nup50-overexpressing vector (Nup50–GFP) and *Kcna4* promoter luciferase vector for 48 h, followed by the detection of luciferase activity. (G) The luminescence intensity of the *Kcna4* promoter in Nup50-knockdown cardiomyocytes. NRVMs were transfected with either scramble siRNA or Nup50 siRNA and *Kcna4* promoter luciferase vector for 48 h, followed by the detection of luciferase activity. Data in E–G are from at least three independent experiments. Data shown are mean±s.d. $^{**}P<0.01$ (unpaired, two-tailed *t*-test for two-group comparisons and one-way ANOVA followed by Tukey's post hoc test for multiple-group comparisons).

Journal of Cell Science (2021) 134, jcs256818. doi:10.1242/jcs.256818

relationship between Nup50 and chromosomes indicates the dynamic interaction in Nup50-mediated regulation of *Kcna4*; therefore, a chromatin immunoprecipitation (ChIP) approach was adopted to verify the interaction between the Nup50 protein and the *Kcna4* gene locus. Our data demonstrated that the DNA segments of the *Kcna4* promoter in Nup50-overexpressing NRVMs were significantly enriched by Nup50 immunoprecipitation compared to the DNA segments of the *Kcna4* gene body (Fig. 3B). The promoter, but not gene body region of *Kcna4* seemed to interact with Nup50 protein. Furthermore, the *Kcna4* promoter region was more enriched in NRVMs overexpressing Nup50 than in those that overexpressed with GFP (Fig. 3C).

Given that the ChIP experiment pulled down DNA fragments of *Kcna4* with higher affinity for Nup50, we selected other ion channel genes (*Scn5a*, *Kcnd3* and *Kcnj2*) and internal genes [β-actin (*Actb*) and *Gapdh*] for Nup50 immunoprecipitation. In line with the results from mRNA and protein examination, while the DNA sequences from the *Kcna4* promoter region were enriched, the genes encoding main ion channels and internal genes in cardiomyocytes were not enriched by the Nup50 antibody (Fig. 3D). Moreover, the DNA fragments from the *Kcna4* promoter region were coimmunoprecipitated with Nup50 protein, but not other nucleoproteins, such as Nup153, Nup107 and Nup54 (Fig. 3E).

To verify whether Nup50 directly binds to the *Kcna4* promoter region, purified Nup50 protein was obtained and mixed with the DNA sequence from the *Kcna4* or *Kcnj2* promoter regions. Following the ChIP procedure, the immunoprecipitated DNA segments were collected to analyze the possible binding region of Nup50 on the *Kcna4* promoter region. Our data showed that while DNA segments from the *Kcna4* or *Kcnj2* promoter regions were not detected upon coimmunoprecipitation with the control protein, there was a concentration of the *Kcna4* promoter region upon *in vitro* ChIP with the Nup50 protein of more than 20 times the concentration of the *Kcna4* promoter region of the input samples. This strongly indicates the direct binding of Nup50 to the *Kcna4* promoter (Fig. 3F). Collectively, Nup50 directly interacts with the promoter region of the *Kcna4* gene in NRVMs.

The FG-repeat domain, but not FG repeats within Nup50, is critically responsible for *Kcna4* transcription in cardiomyocytes

Human Nup50 contains an N-terminal region (aa 1–213), an FG-repeat domain (aa 214–320) and a C-terminal domain (aa 321–468).

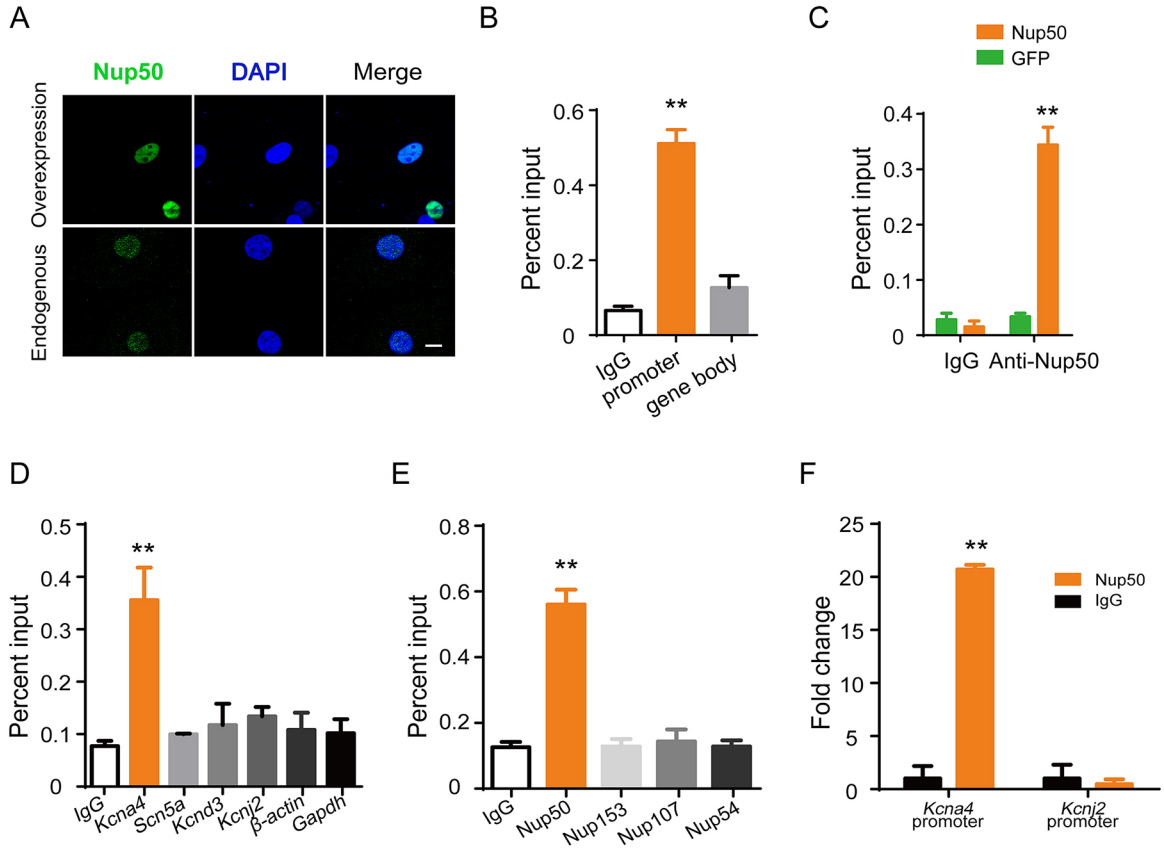

Fig. 3. Direct interaction between Nup50 protein and *Kcna4* promoter. (A) Fluorescence images showing the localization of ectopic Nup50 (upper) and endogenous Nup50 (bottom) in NRVMs. Images are representative of three experiments. Scale bars: 10 µm. (B) Result of the ChIP assay for detecting the interactive region between the Nup50 protein and *Kcna4* gene. (C) Result of the ChIP assay for detecting the interaction between the Nup50 protein and the *Kcna4* promoter region. NRVMs were treated with Nup50 or GFP vector for 48 h, followed by a ChIP assay. ChIP-PCR analysis showed that Nup50, but not GFP, selectively bound the proximal region of the *Kcna4* promoter in NRVMs. (D) The association of Nup50 with the promoter regions of the main ion channel genes (*Scn5a*, *Kcnd3*, *Kcnj2* and *Kcna4*) and internal reference genes (β-actin and *Gapdh*) in NRVMs as measured by ChIP-PCR. (E) The binding of different nucleoporins and the *Kcna4* promoter region. (F) *In vitro* analysis of the physical interaction between the Nup50 protein and the *Kcna4* promoter. Purified Nup50 protein was mixed with *Kcna4* promoter (−2000 to −1) and *Kcnj2* promoter (−2000 to −1) obtained by PCR amplification of rat genomic DNA, and subsequently immunoprecipitated by antibody for ChIP-PCR analysis. Data in B–F are from three independent experiments. Data shown are mean±s.d. $^{**}P<0.01$ (unpaired, two-tailed *t*-test for two-group comparisons and one-way ANOVA followed by Tukey's post hoc test for multiple-group comparisons).

Journal of Cell Science (2021) 134, jcs256818. doi:10.1242/jcs.256818

To identify the domain responsible for *Kcna4* transcription, different truncated variants of Nup50 were constructed and expressed in NRVMs (Fig. 4A). While full-length (FL) Nup50, the N-terminal domain and the mutant with the C-terminal deletion (ΔC-terminus) were localized within the nucleus, the truncated mutants with the N-terminal deletion (ΔN-terminus), the C-terminal domain and the FG-repeat domain showed diffuse distribution in the cytoplasm (Fig. 4B), suggesting that the N-terminus but not the FG-repeat domain or the C-terminal domain is essential for the precise localization of Nup50 in the nucleus. This is consistent with the findings of Buchwalter et al. (2014).

Next, we examined whether it was a transcriptional change that led to the changes in *Kcna4*-encoded Kv1.4 protein expression. To this end, mutants possessing correct nuclear localization, including the N-terminus and the C-terminus-deleted mutant (ΔC-terminus), were overexpressed in NRVMs. We found that, similar to the effects of Nup50-FL overexpression, expression of the ΔC-terminal mutant of Nup50 induced an increase in Kv1.4 protein expression, whereas the N-terminal mutant had no effects (Fig. 4C). In addition, these mutants had no effects on other channel proteins (Fig. S3).

We then measured the luminescence intensity of the *Kcna4* promoter luciferase vector in NRVMs that were co-transfected with the different Nup50 truncation mutants. Overexpression of the N-terminal mutant resulted in a similar value in luminescence intensity to that seen with the mock vector, but the ΔC-terminus

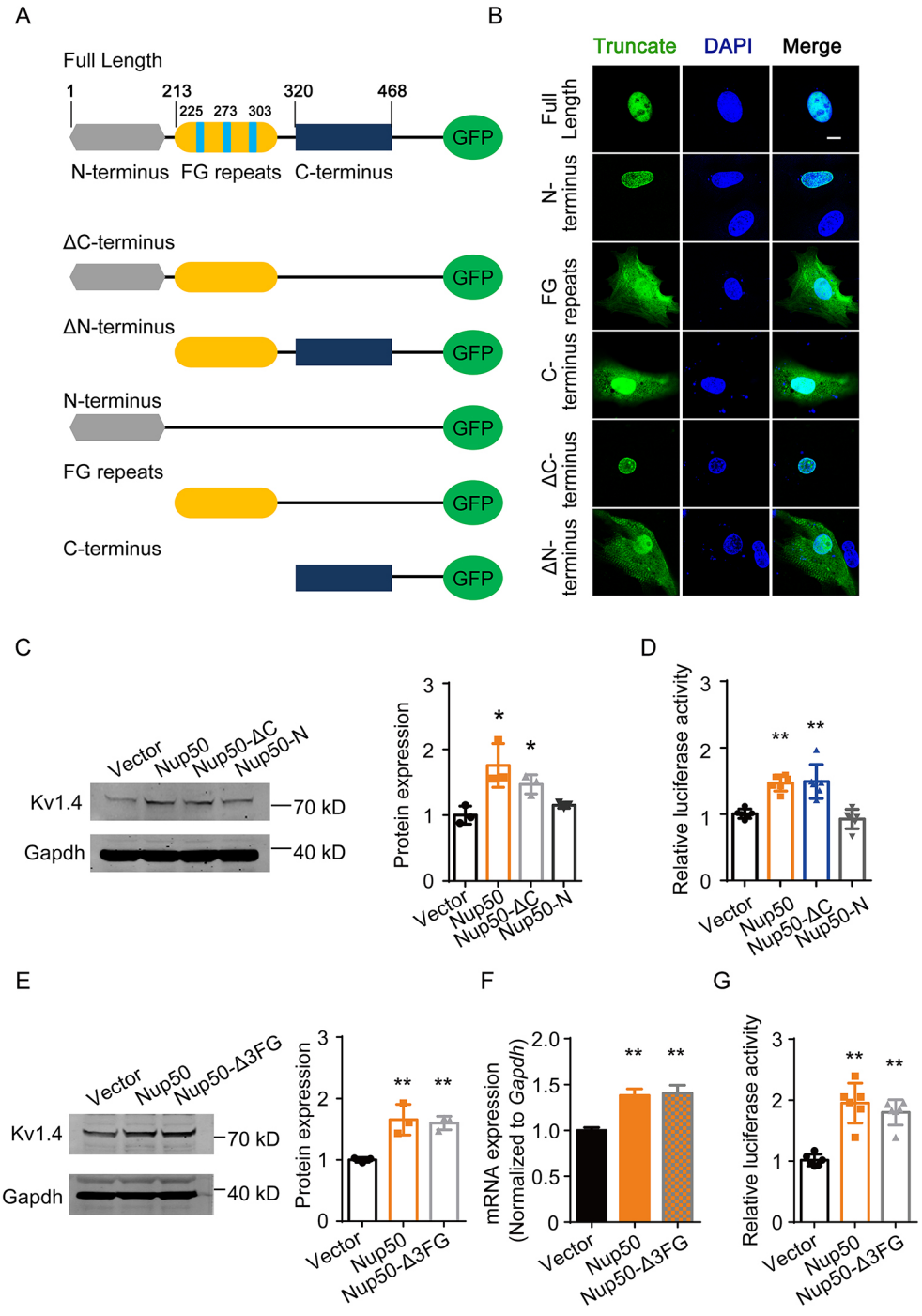

Fig. 4. Identification of the critical domain within Nup50 for *Kcna4* transcription. (A) Schematic diagram of Nup50 truncation mutants used in this study. The different domains of Nup50 protein are indicated. The positions of FG repeats in the FG-repeat domain are indicated in light blue in the full-length diagram. (B) Fluorescence microscopy images of Nup50 mutants in NRVMs. Images are representative of three experiments. Scale bar: 10 µm. (C) Western blotting examination of the effects of Nup50 mutants on Kv1.4 protein expression in NRVMs. NRVMs transfected with different Nup50 truncates for 48 h, followed by the detection of Kv1.4 expression. (D) The luminescence intensity of the *Kcna4* promoter transfected with different Nup50 truncates. NRVMs were transfected with either control vector (GFP) or Nup50 truncates and *Kcna4* promoter luciferase vector for 48 h, followed by the detection of luciferase activity. Western blotting (E) and qPCR analysis (F) showing the effects of the Nup50 mutant with three FG sequence deletions (Nup50-Δ3FG) on the protein and mRNA levels of *Kcna4* in NRVMs. NRVMs were transfected with Nup50-Δ3FG, Nup50-FL or control vector for 48 h, followed by the detection of the protein and mRNA expression of *Kcna4*. (G) The luminescence intensity of the *Kcna4* promoter transfected with Nup50-Δ3FG. NRVMs were transfected with control vector (GFP), Nup50-FL, or Nup50-Δ3FG, and *Kcna4* promoter luciferase reporter for 48 h, followed by the detection of luciferase activity. Data in C–G are from at least three independent experiments. All data are presented as the mean±s.d. **P*<0.05, ***P*<0.01 (unpaired, two-tailed *t*-test for two-group comparisons and one-way ANOVA followed by Tukey's post hoc test for multiple-group comparisons).

Journal of Cell Science (2021) 134, jcs256818. doi:10.1242/jcs.256818

mutant remarkably increased the luminescence intensity (Fig. 4D). These data indicate that the N-terminus of Nup50 is critically required for nuclear localization and that the FG-repeat domain is responsible for the transcriptional activation of the *Kcna4* promoter.

Given that the FG-repeat domain of Nup50 is required for regulating *Kcna4* transcription in cardiomyocytes, we asked whether the 'FG' amino acids within Nup50 are essential for Nup50-mediated regulation. A Nup50 mutant with all three FG sequences deleted (Nup50-Δ3FG) was constructed and transfected into NRVMs. Western blotting and RT-PCR data demonstrated that the expression of *Kcna4* was comparable between Nup50 and the Nup50-Δ3FG mutant in NRVMs (Fig. 4E,F). Then, the dual-luciferase reporter harboring the *Kcna4* promoter was co-transfected with Nup50 or the Nup50-Δ3FG mutant. Consistent with the results for *Kcna4* mRNA and protein, the luminescence activity in the Nup50-Δ3FG mutant group was similar to the luminescence activity in the Nup50 group (Fig. 4G). These results suggest that the FG sequences are dispensable for Nup50-mediated regulation of *Kcna4* expression.

Nup50 enhances the currents of the *KNCA4*-encoded Kv1.4 channel by promoting *KCNA4* transcription

The *Kcna4*-encoded Kv1.4 channel is a prominent member of the Kv1 family (Niwa and Nerbonne, 2010). In the heart, Kv1.4 is distributed in the cardiac ventricular endocardium (Brahmajothi et al., 1999; Xu et al., 1999). Alterations in Kv1.4 expression have been observed in hypertrophy and heart failure, indicating that the behavior of this channel is of particular clinical importance (Tozakidou et al., 2010; Chang et al., 2013; Singhal et al., 2014).

To examine whether Nup50 could affect the function of the Kv1.4 channel, we performed cell electrophysiological analysis. As little *KCNA4* was expressed in HEK293 cells, we adopted a Cas9-mediated technique to transcriptionally activate endogenous Kv1.4 in HEK293 cells (Fig. 5A; Fig. S4A) and recorded Kv1.4 channel currents. Based on a screening strategy, we identified an effective single-guide (sg)RNA targeting the human *KCNA4* promoter, which achieved a more than 20-fold elevation in *KCNA4* mRNA and a marked Kv1.4 protein increase in HEK293 cells (Fig. S4B,C). The endogenous production of mRNA was unique for *KCNA4* without any effect on other ion channel-encoding genes such as *SCN5A*, *CACNA1C*, *KCNQ1* and *HERG* (Fig. S4D). In addition, the transcriptional activation of *KCNA4* resulted in the production of Kv1.4 channel currents in HEK293 cells. The electrophysiological properties of the currents generated by endogenous activation in HEK293 cells were similar to the electrophysiological properties of the currents generated by Kv1.4 vector overexpression.

Using the above cell model of endogenous *KCNA4* activation, we investigated the potential roles of Nup50-mediated transcription of endogenous *KCNA4* genes. dCas9-VP64- and *KCNA4*-targeted sgRNAs were co-transfected with Nup50 or control vector, followed by qRT-PCR analysis at 48 h post transfection. Our data showed that Nup50 enhanced the transcription of endogenous human *KCNA4* by an ∼4-fold increase in the mRNA level (Fig. 5B) and subsequently increased the expression of *KCNA4*-encoded Kv1.4 channel proteins (Fig. 5C). Functional analysis with whole-cell voltage clamp recordings demonstrated that the current density of the voltage-gated Kv1.4 channel was increased in Nup50-overexpressing HEK293 cells with endogenous *KCNA4* activation

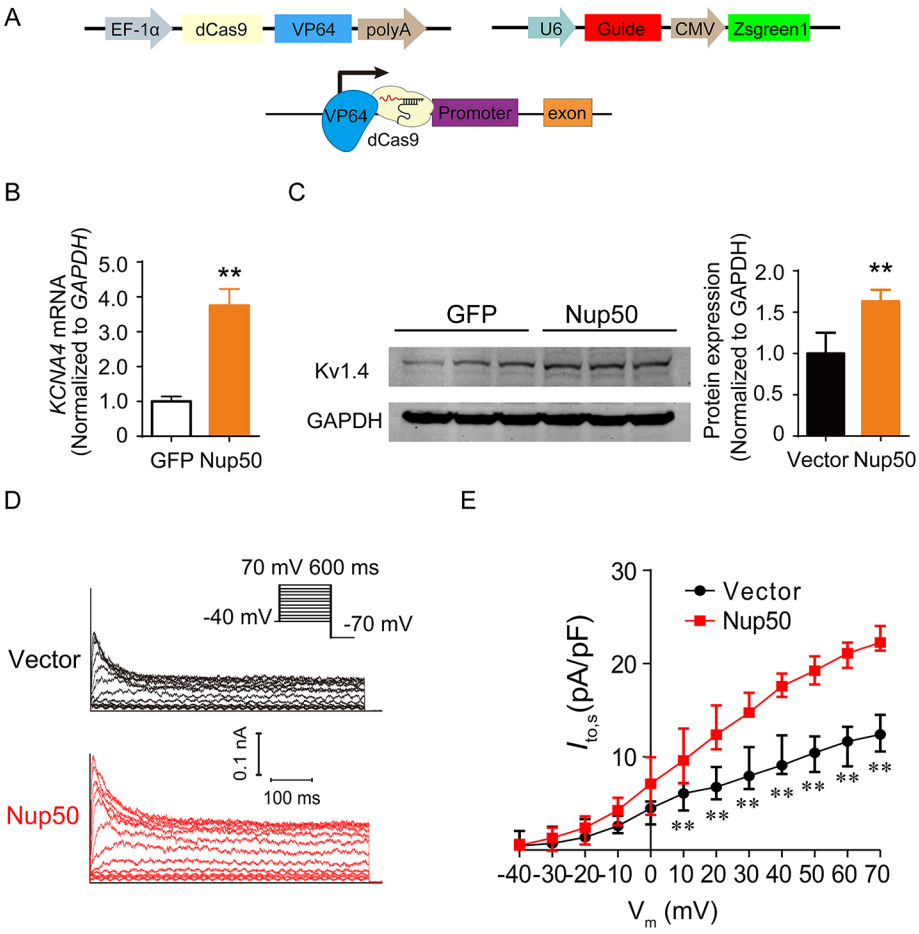

Fig. 5. Effects of Nup50 on endogenous Kv1.4 currents in HEK293 cells. (A) Schematic illustration of activating endogenous *KCNA4* in HEK293 cells. Top, the construct with the dCas9-VP64 fused protein (top left) and gRNA (top right); bottom, Cas9-mediated transcriptional activation by using dCas9 and the activation domain (VP64) at the transcriptional start site of *KCNA4* gene. (B) The mRNA level of *KCNA4* transfected with either control vector (GFP) or Nup50–GFP vector in HEK293 cells transfected with dCas9/*KCNA4*-gRNA. Data are shown as the mean±s.d. (n=3 independent transfections). (C) Western blotting showing the expression of Kv1.4 in Nup50-overexpressing HEK293 cells transfected with dCas9-VP64 fusion protein and *KCNA4*-gRNA. Data are mean±s.d. from three independent experiments. (D) Representative K^+ currents recorded from HEK293 cells transfected with dCas9-VP64 and *KCNA4* targeting gRNA plus either control vector (GFP) or Nup50. Currents were recorded with the whole-cell patch-clamp technique. Cells were held at −70 mV, and $I_{to,s}$ was elicited by a family of voltage steps to potentials ranging from −40 to +70 mV with 10 mV increments. (E) Current–voltage relationship of $I_{to,s}$ in HEK293 cells transfected with dCas9-VP64 and *KCNA4* targeting gRNA plus either control vector (GFP) (n=7) or Nup50 (n=20). Currents were normalized to cell capacity. Data are mean±s.e.m. **P<0.01 (unpaired two-tailed t-test).

Journal of Cell Science (2021) 134, jcs256818. doi:10.1242/jcs.256818

(Fig. 5D,E). The average peak outward current in the Nup50-overexpression group exhibited a greater value (+70 mV, 22.37 pA/pF, n=20) than the average peak outward current in the control vector group (12.62 pA/pF at +70 mV, n=7, P<0.01). By contrast, expression of another nucleoporin, Nup153 had no effect on the currents of the voltage-gated Kv1.4 channel in HEK293 cells with endogenous *KCNA4* activation (Fig. S5). Collectively, these results show that Nup50 can increase the amplitude of endogenous Kv1.4 channels by targeting the *Kcna4* promoter.

Nup50-mediated regulation of the *Kcna4*-encoded Kv1.4 channel in cardiac myocytes and tissues

To determine whether Nup50-mediated regulation of Kv1.4 occurs in cardiomyocytes, we performed an electrophysiological experiment in NRVMs. Considering that two different I_{to} channels, $I_{to,f}$ (mediated by Kv4.2 and Kv4.3 channels) and $I_{to,s}$ (mediated by the Kv1.4 channel), have been distinguished in rat ventricular myocytes, we used heteropodatoxin, a peptide isolated from spider venom, to specifically block Kv4.2 and Kv4.3 K^+ channels (Sanguinetti et al., 1997; Zarayskiy et al., 2005). Our whole-cell voltage clamp recordings demonstrated that the current density of $I_{to,s}$ was dramatically decreased in Nup50-depleted NRVMs compared with the negative control group (Fig. 6A,B). The average peak outward current in Nup50-depleted myocytes showed a decreased value (+60 mV, 9.13 pA/pF, n=25) compared with the control (15.36 pA/pF at +60 mV, n=15, P<0.01). Taken together, the absence of Nup50 attenuates the amplitude of $I_{to,s}$ currents in cardiomyocytes.

Cardiac arrhythmias following ischemic compromise of the heart are a major cause of death after myocardial infarction. To further explore the potential contribution of Nup50-mediated regulation on the expression and function of the *Kcna4*-encoded Kv1.4 channel in cardiac arrhythmias, we examined the mRNA expression of Nup50 and *Kcna4* in a rat model of acute myocardial infarction. Strikingly, a concomitant increase in the mRNA levels of Nup50 and *Kcna4* was observed at 72 h after myocardial infarction (Fig. 6C). Furthermore, the elevation in Kv1.4 protein was accompanied by an increase in the Nup50 protein (Fig. 6D). These results suggest that the Nup50-dependent regulation of *Kcna4*-encoded Kv1.4 channel protein expression is relevant to ischemic cardiac diseases *in vivo*.

DISCUSSION

A large body of evidence has demonstrated that nucleoporins have functions of beyond nucleocytoplasmic transport. Nucleoporins also play active roles in gene expression, RNA stabilization and post-transcriptional regulation. Nup50, classified as a nuclear basket nucleoporin, has been shown to ferry cargos across the NPC into the nuclear interior. The present study identifies Nup50 as a transcription activator in *Kcna4* expression. Of importance, the response of Nup50 to transcription activation was specific to *Kcna4*, and this effect of Nup50 is independent of the well-known roles in nuclear transport.

Structurally, Nup50 is a critical member of the nuclear basket consisting of Nup50, Nup153 and TPR. Interestingly, the components of the nuclear basket are not similar to the components of cytoplasmic filaments. This asymmetric distribution of nucleoporins underlies the differential functions in the cytoplasmic and nuclear faces of NPCs. Among the C-terminal domain, FG-repeat and N-terminal domain of the Nup50 protein, we revealed that the N-terminal segment of Nup50 is required for its nucleoplasmic localization, whereas the FG-repeat and the C-terminal modules of Nup50 seem to be dispensable for the intranuclear distribution (Fig. 4A,B).

For the activation of *Kcna4* expression, the truncated mutant of Nup50 lacking the C-terminus is sufficient to activate *Kcna4*

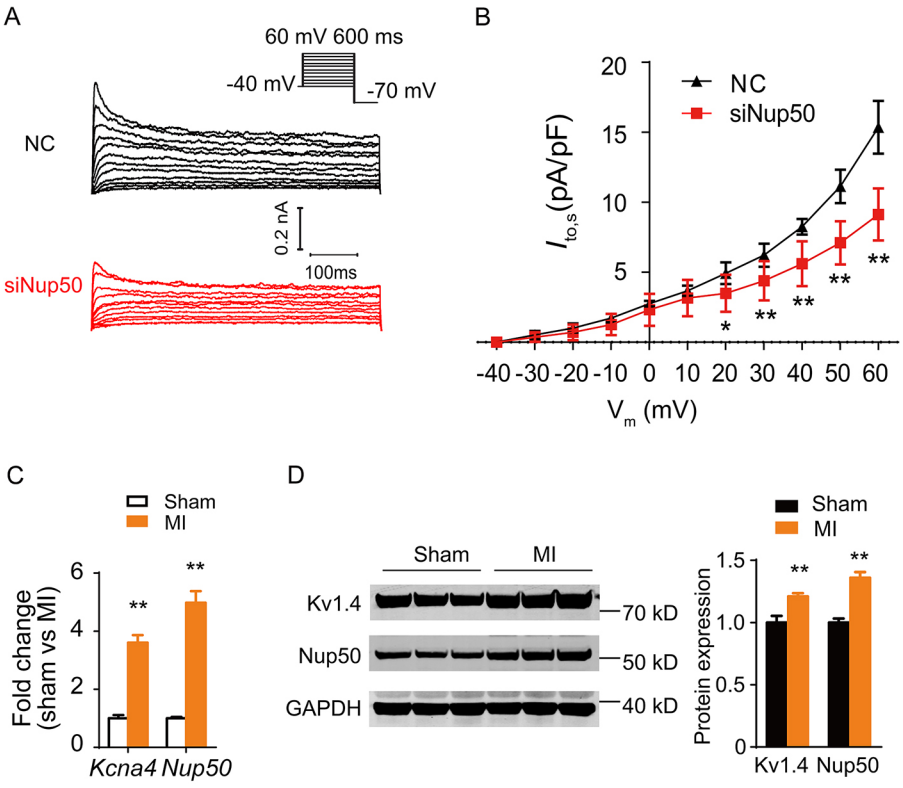

Fig. 6. Effects of Nup50 on cardiac $I_{to,s}$ currents and pathological implications. (A) Representative K^+ currents recorded from NRVMs transfected with either NC or Nup50 siRNA. The cells were held at −70 mV, and $I_{to,s}$ was elicited by a family of voltage steps to potentials ranging from −40 to +60 mV with 10 mV increments. HpTX2 was added to block the current of $I_{to,f}$. (B) Current–voltage relationship of $I_{to,s}$ in NRVMs. The cells were transfected with either NC (n=15) or Nup50 siRNA (n=25) for 48 h, followed by electrophysiological analysis. Currents were normalized to cell capacity. Data are mean±s.e.m. (C) The mRNA levels of Nup50 and *Kcna4* in rat ventricular tissues 3 days after acute myocardial infarction. Data are presented as the mean±s.d. of four independent experiments. (D) Protein expression levels of Nup50 and Kv1.4 in ischemic ventricular tissues from the rat model of acute myocardial infarction. Data in D are mean±s.d. from three independent experiments *P<0.05, **P<0.01 (unpaired two-tailed t-test).

transcription, while the N-terminus of Nup50 has no effect. The FG-repeat domain is a prominent feature of NPCs, serving as docking sites for transport receptors (Nakielny and Dreyfuss, 1999; Ben-Efraim and Gerace, 2001) or diffusion barriers between the cytoplasm and nuclear compartments (Frey et al., 2006). There were five 'FG' sequences found in full-length Nup50, two in the N-terminus and three in the FG-repeat domain. The N-terminal domain is necessary for Nup50 localization and Nup153 binding (Makise et al., 2012), and the FG-repeat domain appears to function in transcription activation. This unique FG-repeat domain not only forms the NPC diffusion barrier and serves as a specific binding site for nuclear transport factors but is also associated with gene transcription (Kasper et al., 1999). However, when we deleted the three FG repeat sequences in the FG-repeat domain, the transcriptional effects of Nup50 remained (Fig. 4E–G), which implies that the FG sequences are critical for nucleocytoplasmic transport but may be dispensable for transcriptional activation. The exact composition and specific sequence motifs of FG repeats vary between nucleoporins and species, indicating that each nucleoporin could function differently.

Nup50 engages in transcriptional regulation and development. Not all the functions of Nup50 are required for nucleocytoplasmic transport. In nucleocytoplasmic transport, Nup50 is thought to be a 'tristable switch' due to its ability to interact with importin-α, importin-β and Ran (Lindsay et al., 2002), but our data show that the transporting function may not be associated with transcription activation. The truncation of the C-terminal domain of Nup50, which interacts with Ran, did not affect the transcriptional activity of Nup50 (Fig. 4D). Our immunofluorescence data showed that Nup50 was distributed broadly throughout the nucleoplasm and interacted dynamically with euchromatin. The promoter region of *Kcna4* was significantly enriched by Nup50 ChIP. Although the N-terminus of Nup50 is required for transcriptional activation, Nup153 is not necessary. Moreover, Nup153 did not regulate the expression of *Kcna4* (Fig. 1F). These findings were consistent with a previous report showing that the behavior of Nup50 is dependent on active transcription by RNA polymerase II and requires the N-terminal half of the protein and is independent of importin-α, Nup153 and Nup98 (Buchwalter et al., 2014). Additionally, a genetic study has reported a new biological profile of Nup50 in which Nup50-deficient fibroblasts proliferate normally but $Nup50^{-/-}$ mice die late in gestation (Smitherman et al., 2000). These findings suggest that Nup50 may play an essential role in particular cell types during development and in transcriptional regulation.

The Nup50-mediated transcriptional regulation of ion channels in cardiac myocytes is specific. Among the major ion channels related to electrical activity in cardiomyocytes, the *Kcna4*-encoded Kv1.4 channel is the only channel regulated by Nup50. The *Kcna4* gene encodes the α-subunit critical for the Kv1.4 channel, which in turn yields the slowly inactivating transient outward K^+ currents in the repolarization phase of the action potential duration. The interaction between Nup50 and the *Kcna4* promoter sequence establishes a modular basis for the functional selectivity of Nup50. The mechanisms responsible for Nup50-specific regulation of this gene have yet to be determined. Evidence has shown that the *Kcna4* promoter is GC-rich, contains three SP1 repeats, and lacks canonical TATAAA and GGCAATCT motifs (Wymore et al., 1996), which may provide a clue for further study. Our experiments cannot rule out the possibility that Nup50 also modulates the transcription of genes other than ion channels. Nup50 ChIP sequencing may provide more information on the downstream genes and specific regulatory motifs. Among the nucleoporins, Nup50 seems not to be the only one that can regulate the expression of *Kcna4*. Our additional experiment suggests the possibility of new candidate genes for *Kcna4* transcriptional regulation (Fig. S6).

As it is responsible for the major component of $I_{to,s}$, the *Kcna4*-encoded channel plays an important role in the repolarization of cardiac myocytes. The expression of *Kcna4* at the mRNA and protein levels was increased remarkably 3 days after myocardial infarction, paralleling the risky time window of cardiac arrhythmias. Evidence has shown the existence of gene isoform switching in K^+ ion channels under pathological conditions. For example, isoform switching from Kv4.2 to Kv1.4 is indicated as the mechanism underlying the slower kinetics of transient outward K^+ current observed in the diabetic ventricle (Nishiyama et al., 2001). Therefore, the elevation of Nup50 and *Kcna4* induced by myocardial infarction may be an adaptive response to ischemic injury.

In summary, our findings clarify for the first time the mechanism by which Nup50 transcriptionally regulates the *Kcna4*-encoded Kv1.4 channel expression and thus $I_{to,s}$ currents, which may elucidate the control of bioelectrical activity in ischemic cardiac diseases.

MATERIALS AND METHODS

Cell culture

Neonatal rat ventricle myocytes (NRVMs) were isolated from hearts of 2-day-old Sprague-Dawley rats, and cultured in Dulbecco's modified Eagle's medium (DMEM) medium containing 10% fetal bovine serum (FBS) and 100 µM BrdU for 16–24 h and maintained in DMEM containing 10% FBS, 2 mM L-glutamine and 1% penicillin and streptomycin (Gibco, Invitrogen, Carlsbad, USA). All animal experiments were performed according to approved guidelines. HEK293 cells (ATCC) were cultured in DMEM with 10% FBS and 1% penicillin/streptomycin.

Transfection and plasmids

siRNA duplexes, designed and synthesized by GenePharma (Shanghai, China), were transfected individually at 50 nM using the Lipofectamine RNAiMAX transfection reagent (13778-100, Thermo Fisher Scientific, Shanghai, China) according to the manufacturer's instructions. The sequences of siRNAs used in this study are listed in Table S1. The scrambled duplex provided by GenePharma was used as the negative control (NC) for all knockdown experiments.

Various truncation mutants of Nup50, including GFP-tagged Nup50-full length (FL, 1–468 aa), Nup50-N-terminus domain (1–213 aa), Nup50-FG-repeats domain (214–320 aa), Nup50-C-terminus domain (321–468 aa), Nup50 truncates lacking the N-terminal domain (Nup50-ΔN-terminus) or lacking the C-terminal domain (Nup50-ΔC-terminus) were constructed by amplifying the corresponding truncations. For the functional analysis of the 'FG' sequences within Nup50, the DNA sequence of the FG-repeats domain with three 'FG' sequences deleted was synthesized and inserted between the N-terminal and C-terminal domains of Nup50 (Nup50-Δ3FG). For the validation of the effects of Nup50 on the *Kcna4* expression, a Myc-tagged Nup50 and Nup153 were constructed by amplifying the full length of coding sequences and inserting these into the pDC316 vector (Microbix Biosystems, Toronto, ON) with the Myc tag at the N-terminus. All the constructs were verified by Sanger sequencing.

Transient plasmid transfections were performed with Lipofectamine 3000 (Invitrogen, Carlsbad, CA, USA) according to the manufacturer's protocol.

Real-time RT-PCR

Total RNA was isolated with Trizol (Invitrogen) and quantified by RT-PCR (RR037A, TaKaRa, Kyoto, Japan). The quantification of mature mRNA was conducted by using an oligo-dT primer. The mRNA quantification was conducted utilizing SYBR Green-based detection technology. Primers were designed with Primer Express (Applied Biosystems), and the sequences are listed in Table S2. The expression level of the target mRNA was normalized

to the expression of the internal references, and calculated using the method of $2^{-(\Delta\Delta Ct)}$.

Myocardial infarction

Myocardial infarction was performed in female Sprague-Dawley rats. Briefly, rats were lightly anesthetized with 10% chloral hydrate (0.3 ml/100 g), intubated, and then ventilated with a rodent respirator. The chest cavity was opened via left thoracotomy. Myocardial infarction was induced by ligation of the left anterior descending artery (LAD) with a 6-0 silk suture at the site of its emergence from the left atrium. The sham-operated animals underwent the same procedure without LAD ligation. At the day 3, the surviving animals were killed, and their hearts were quickly excised and rapidly frozen in liquid nitrogen. The RNA and protein were extracted from the infarcted and non-infarcted region of the left ventricle of myocardial infarction or control rats for the detection of *Kcna4* and Nup50 expression.

Western blotting

Cells were lysed in RIPA buffer (Beyotime, Zhejiang, China) containing protease inhibitor cocktail tablets (Roche Applied Science, Mannheim, Germany). Proteins were separated by SDS-PAGE (Invitrogen) and transferred onto PVDF membranes. The membranes were incubated at room temperature for 1 h with 5% non-fat milk, followed by incubation with antibodies against Kv1.4 (1:1000, 19697-1-AP, ProteinTech Group, Wuhan, Hubei, China), Nup50 (1:1000, 20798-1-AP, ProteinTech Group, Wuhan, Hubei, China), Myc (1:1000; #2272, Cell Signaling Technology, Danvers, MA, USA), β-actin (1:10,000; 60008-1-Ig, ProteinTech Group) and GAPDH (1:5000; Beyotime, Zhejiang, China) at 4°C overnight. After washing, blots were treated with the appropriate IRDye 800 (LI-COR Biosciences, Lincoln, NE, USA) conjugated secondary antibody (1:10,000; Gaithersburg, MD, USA) at room temperature for 1 h. Images were recorded using the Odyssey infrared imaging system and analyzed using the Odyssey Application Software v2 (LI-COR Biosciences).

Luciferase reporter assay

For the functional analysis of *Kcna4* promoter, the sequences of *Kcna4* promoter (−2000 to −1, −2000 to −1001 and −1000 to −1) was amplified from the rat genomic DNA and inserted into the 5′ upstream of the *Renilla* luciferase gene in psiCheck2 (Promega, Madison, WI, USA) to substitute for the original SV40 promoter. The resultant psiCheck2-promoter constructs were co-transfected with Nup50-FL or its truncates. At 48 h after transfection, the firefly and *Renilla* luciferase activities were analyzed using the dual-luciferase reporter assay system (Promega, Madison, WI, USA).

Fluorescent imaging

NRVMs transfected with Nup50-FL or its different truncates were cultured on coverslips for 48 h, followed by the fixation in 4% (w/v) paraformaldehyde for 15 min. Nuclei were counterstained with ToPro3 (Molecular Probes, Eugene, OR, USA). Cell images were obtained using a Leica SP5 confocal microscope with a 63× objective lens. For endogenous Nup50 immunofluorescent staining, NRVMs were grown at low density on coverslips and maintained for 2 days. Cells were fixed with 4% paraformaldehyde, permeabilized with 0.05% Triton X-100 and incubated with primary antibody against Nup50 (1:100, ab151567, abcam) at 4°C overnight. Cells were washed three times and incubated for 1 h at room temperature with goat anti-rabbit-IgG secondary antibody conjugated to Alexa Fluor 488 (1:1000, ab150077, abcam). The nuclei were visualized by DAPI staining (D9542, Sigma), and the fluorescence images were recorded on a Leica SP8 confocal microscope.

dCas9/sgRNA vectors

The dCas9-effector plasmid pLenti-dCAS-VP64_Blast was obtained from Addgene (plasmid #61425) (Konermann et al., 2015). For the flexible insertion of sgRNA sequences and easy trace of transfected cells, the sequence containing BsmBI enzyme sites and gRNA scaffold was cloned between the BamHI and EcoRI of pLVX-shRNA2 (632179, Clontech Laboratories, Takara, Japan) by using the ClonExpress® II One Step Cloning Kit (C112-02, Vazyme Biotech, Nanjing, Jiangsu, China). The resultant construct pLVX-U6-BsmBI-Zsgreen1 was verified by Sanger sequencing and is listed in Fig. S2. The gRNAs for endogenous human *KCNA4* activation were selected to bind the 1–1000 nt upstream of the transcriptional start site. To clone the guide sequence into the vector, two oligonucleotides harboring the gRNA sequences were synthesized and ligated between the two BsmBI sites. The sequences for gRNAs are listed in Table S3.

ChIP and *in vitro* binding assay

ChIP was performed using SimpleChIP Plus Enzymatic Chromatin IP Kit (Magnetic Beads) (#9005, Cell Signaling Technology) according to the manufacturer's instructions. NRVMs transfected with Nup50–GFP and control vector (GFP) were cultured in 10-cm culture dishes and were fixed with 37% formaldehyde to cross-link proteins and DNA (1% final concentration). Then the chromatin was digested with micrococcal nuclease (#10011, Cell Signaling Technology) into 150–900 bp DNA/protein fragments. Nup50 antibody (ab151567, abcam) was added, and the complex was captured by Protein G magnetic beads, and thereafter the immunoprecipitated chromatin was decross-linked. The recruited DNA was subjected to a real-time PCR reaction. The qPCR data from the IPs were normalized to the values of the same input sample. Primer sequences used for ChIP are listed in Table S2.

For the *in vitro* binding assays, recombinant GST–Nup50 protein was purchased from Novus (H00010762-P01, Novus Biologicals, Littleton, CO, USA). The DNA sequences of *Kcna4* and *Kcnj2* promoter regions (−2000 to −1) were obtained by the amplification of rat genomic DNA and purified by gel extraction. The DNA sequences of *Kcna4* promoter or *Kcnj2* promoter were mixed with Nup50 protein and immunoprecipitated with GST antibody (5 µg/reaction, ab19256, abcam) according to the manufacturer's instructions.

Electrophysiological recording

A standard whole-cell patch-clamp technique was used to measure the transient outward K^+ channel current, $I_{to,s}$ at room temperature (22–24°C) (EPC-10, HEKA Elecktronik, Lambrecht, Germany). Borosilicate-glass electrodes with a tip resistance of 2–5 MΩ were used. The $I_{to,s}$ current was expressed as the current density normalized to the cell capacitance. The extracellular (bath) solution contained (mmol/l): 140 NaCl, 4 KCl, 2 $CaCl_2$, 1 $MgCl_2$, and 10 HEPES, pH adjusted to 7.4 with NaOH. The pipette solution contained (mmol/l): 110 KCl, 31 KOH, 10 EDTA, 5.17 $CaCl_2$, 1.42 $MgCl_2$, 4 MgATP and 10 HEPES, pH adjusted to 7.2 with KOH.

To measure the $I_{to,s}$ current in HEK293 cells, the cell was held at −70 mV. The $I_{to,s}$ current was recorded in HEK293 cells elicited by step depolarization of 600 ms duration to +70 mV from a holding potential of −40 mV in 10 mV increments, separated by a 1-s test interval at the holding potential of −70 mV.

The $I_{to,s}$ current from transfected NRVMs was recorded as described previously (Kassiri et al., 2002; Deschênes et al., 2008). The pipette solution contained (mM): KCl 45, K-aspartate 85, Na-pyruvate 5, MgATP 5.0, EGTA 10, HEPES 10, and glucose 11, pH adjusted to 7.3 with KOH; the extracellular solution contained (mM): NaCl 135, KCl 5.4, $CaCl_2$ 1.8, $MgCl_2$ 1, NaH_2PO_4 0.33, HEPES 10, and glucose 10, pH adjusted to 7.2 with NaOH. $I_{to,s}$ was elicited by depolarization steps from −40 mV to +60 mV in 10 mV increments with a 1-s test interval. $I_{Ca,L}$ and I_{Na} were eliminated by 10 µM nifedipine (Alomone Labs, Jerusalem, Israel) and 30 µM tetrodotoxin (TTX; Alomone Labs, Jerusalem, Israel) included in the recording solution. Heteropodatoxin-2 (HpTX2, 2 uM) (ab141874, abcam) was added to block $I_{to,f}$ current. A brief 30-ms prepulse to −40 mV was used at the beginning of the protocol to eliminate the Na^+ current (I_{Na}).

Statistical analysis

All electrophysiological data are expressed as the means±s.e.m., and other quantitative data are presented as the mean±s.d. Differences were analyzed using an unpaired two-tailed *t*-test for the two groups and by a one-way ANOVA followed by Tukey's post hoc test for multiple groups. The results were considered statistically significant if $P<0.05$.

Competing interests
The authors declare no competing or financial interests.

Author contributions
Conceptualization: L.X., Y.S.; Methodology: X.G., S.Y., Y.G.; Validation: X.G., S.Y., Y.G.; Formal analysis: X.G., S.Y.; Investigation: L.X.; Data curation: X.G., S.Y.; Writing - original draft: X.G., S.Y.; Writing - review & editing: L.X.; Visualization: S.Y., Y.G.; Supervision: L.X., Y.S.; Funding acquisition: L.X., Y.S.

Funding
This work was funded by the Grants from the National Key Research and Development Plan of China (2018YFC1312504 to L.X.), Key Disciplines Group Construction Project of Pudong Health Bureau of Shanghai (PWZxq2017-05), Top-level Clinical Discipline Project of Shanghai Pudong District (PWYgf2018-02), the Natural Science Foundation of Jiangxi Province of China (20192BAB205006 to Y.S.).

References
Beck, M. and Hurt, E. (2017). The nuclear pore complex: understanding its function through structural insight. *Nat. Rev. Mol. Cell Biol.* **18**, 73-89. doi:10.1038/nrm.2016.147

Ben-Efraim, I. and Gerace, L. (2001). Gradient of increasing affinity of importin β for nucleoporins along the pathway of nuclear import. *J. Cell Biol.* **152**, 411-418. doi:10.1083/jcb.152.2.411

Brahmajothi, M. V., Campbell, D. L., Rasmusson, R. L., Morales, M. J., Trimmer, J. S., Nerbonne, J. M. and Strauss, H. C. (1999). Distinct transient outward potassium current (I_{to}) phenotypes and distribution of fast-inactivating potassium channel alpha subunits in ferret left ventricular myocytes. *J. Gen. Physiol.* **113**, 581-600. doi:10.1085/jgp.113.4.581

Buchwalter, A. L., Liang, Y. and Hetzer, M. W. (2014). Nup50 is required for cell differentiation and exhibits transcription-dependent dynamics. *Mol. Biol. Cell* **25**, 2472-2484. doi:10.1091/mbc.e14-04-0865

Chang, S.-L., Chen, Y.-C., Hsu, C.-P., Kao, Y.-H., Lin, Y.-K., Lai, Y.-J., Yeh, H.-I., Higa, S., Chen, S.-A. and Chen, Y.-J. (2013). Heat shock protein inducer modifies arrhythmogenic substrate and inhibits atrial fibrillation in the failing heart. *Int. J. Cardiol.* **168**, 4019-4026. doi:10.1016/j.ijcard.2013.06.072

Deschênes, I., Armoundas, A. A., Jones, S. P. and Tomaselli, G. F. (2008). Post-transcriptional gene silencing of KChIP2 and Navβ1 in neonatal rat cardiac myocytes reveals a functional association between Na and I_{to} currents. *J. Mol. Cell. Cardiol.* **45**, 336-346. doi:10.1016/j.yjmcc.2008.05.001

Frey, S., Richter, R. P. and Görlich, D. (2006). FG-rich repeats of nuclear pore proteins form a three-dimensional meshwork with hydrogel-like properties. *Science* **314**, 815-817. doi:10.1126/science.1132516

Guan, T., Kehlenbach, R. H., Schirmer, E. C., Kehlenbach, A., Fan, F., Clurman, B. E., Arnheim, N. and Gerace, L. (2000). Nup50, a nucleoplasmically oriented nucleoporin with a role in nuclear protein export. *Mol. Cell. Biol.* **20**, 5619-5630. doi:10.1128/MCB.20.15.5619-5630.2000

Kasper, L. H., Brindle, P. K., Schnabel, C. A., Pritchard, C. E. J., Cleary, M. L. and van Deursen, J. M. A. (1999). CREB binding protein interacts with nucleoporin-specific FG repeats that activate transcription and mediate NUP98-HOXA9 oncogenicity. *Mol. Cell. Biol.* **19**, 764-776. doi:10.1128/MCB.19.1.764

Kassiri, Z., Hajjar, R. and Backx, P. H. (2002). Molecular components of transient outward potassium current in cultured neonatal rat ventricular myocytes. *J. Mol. Med.* **80**, 351-358. doi:10.1007/s00109-002-0325-7

Knockenhauer, K. E. and Schwartz, T. U. (2016). The nuclear pore complex as a flexible and dynamic gate. *Cell* **164**, 1162-1171. doi:10.1016/j.cell.2016.01.034

Konermann, S., Brigham, M. D., Trevino, A. E., Joung, J., Abudayyeh, O. O., Barcena, C., Hsu, P. D., Habib, N., Gootenberg, J. S., Nishimasu, H. et al. (2015). Genome-scale transcriptional activation by an engineered CRISPR-Cas9 complex. *Nature* **517**, 583-588. doi:10.1038/nature14136

Lindsay, M. E., Plafker, K., Smith, A. E., Clurman, B. E. and Macara, I. G. (2002). Npap60/Nup50 is a tri-stable switch that stimulates importin-alpha:beta-mediated nuclear protein import. *Cell* **110**, 349-360. doi:10.1016/s0092-8674(02)00836-x

Ling, D. and Salvaterra, P. M. (2011). Robust RT-qPCR data normalization: validation and selection of internal reference genes during post-experimental data analysis. *PLoS ONE* **6**, e17762. doi:10.1371/journal.pone.0017762

Makise, M., Mackay, D. R., Elgort, S., Shankaran, S. S., Adam, S. A. and Ullman, K. S. (2012). The Nup153-Nup50 protein interface and its role in nuclear import. *J. Biol. Chem.* **287**, 38515-38522. doi:10.1074/jbc.M112.378893

Matsuura, Y. and Stewart, M. (2005). Nup50/Npap60 function in nuclear protein import complex disassembly and importin recycling. *EMBO J.* **24**, 3681-3689. doi:10.1038/sj.emboj.7600843

Moore, M. S. (2003). Npap60: a new player in nuclear protein import. *Trends Cell Biol.* **13**, 61-64. doi:10.1016/S0962-8924(02)00044-2

Nakielny, S. and Dreyfuss, G. (1999). Transport of proteins and RNAs in and out of the nucleus. *Cell* **99**, 677-690. doi:10.1016/S0092-8674(00)81666-9

Nishiyama, A., Ishii, D. N., Backx, P. H., Pulford, B. E., Birks, B. R. and Tamkun, M. M. (2001). Altered K^+ channel gene expression in diabetic rat ventricle: isoform switching between Kv4.2 and Kv1.4. *Am. J. Physiol. Heart Circ. Physiol.* **281**, H1800-H1807. doi:10.1152/ajpheart.2001.281.4.H1800

Niwa, N. and Nerbonne, J. M. (2010). Molecular determinants of cardiac transient outward potassium current (I_{to}) expression and regulation. *J. Mol. Cell. Cardiol.* **48**, 12-25. doi:10.1016/j.yjmcc.2009.07.013

Nofrini, V., Di Giacomo, D. and Mecucci, C. (2016). Nucleoporin genes in human diseases. *Eur. J. Hum. Genet.* **24**, 1388-1395. doi:10.1038/ejhg.2016.25

Ogawa, Y., Miyamoto, Y., Asally, M., Oka, M., Yasuda, Y. and Yoneda, Y. (2010). Two isoforms of Npap60 (Nup50) differentially regulate nuclear protein import. *Mol. Biol. Cell* **21**, 630-638. doi:10.1091/mbc.e09-05-0374

Raices, M. and D'Angelo, M. A. (2012). Nuclear pore complex composition: a new regulator of tissue-specific and developmental functions. *Nat. Rev. Mol. Cell Biol.* **13**, 687-699. doi:10.1038/nrm3461

Sanguinetti, M. C., Johnson, J. H., Hammerland, L. G., Kelbaugh, P. R., Volkmann, R. A., Saccomano, N. A. and Mueller, A. L. (1997). Heteropodatoxins: peptides isolated from spider venom that block Kv4.2 potassium channels. *Mol. Pharmacol.* **51**, 491-498.

Singhal, R., Chang, S.-L., Chong, E., Hsiao, Y.-W., Liu, S.-H., Tsai, Y.-N., Hsu, C.-P., Lin, Y.-J., Lo, L.-W., Ha, T. L. et al. (2014). Colchicine suppresses atrial fibrillation in failing heart. *Int. J. Cardiol.* **176**, 651-660. doi:10.1016/j.ijcard.2014.07.069

Smitherman, M., Lee, K., Swanger, J., Kapur, R. and Clurman, B. E. (2000). Characterization and targeted disruption of murine Nup50, a $p27^{Kip1}$-interacting component of the nuclear pore complex. *Mol. Cell. Biol.* **20**, 5631-5642. doi:10.1128/MCB.20.15.5631-5642.2000

Tarazón, E., Rivera, M., Roselló-Lletí, E., Molina-Navarro, M. M., Sánchez-Lázaro, I. J., España, F., Montero, J. A., Lago, F., González-Juanatey, J. R. and Portolés, M. (2012). Heart failure induces significant changes in nuclear pore complex of human cardiomyocytes. *PLoS ONE* **7**, e48957. doi:10.1371/journal.pone.0048957

Tozakidou, M., Goltz, D., Hagenström, T., Budack, M. K., Vitzthum, H., Szlachta, K., Bähring, R. and Ehmke, H. (2010). Molecular and functional remodeling of I_{to} by angiotensin II in the mouse left ventricle. *J. Mol. Cell. Cardiol.* **48**, 140-151. doi:10.1016/j.yjmcc.2009.08.027

Wymore, R. S., Negulescu, D., Kinoshita, K., Kalman, K., Aiyar, J., Gutman, G. A. and Chandy, K. G. (1996). Characterization of the transcription unit of mouse Kv1.4, a voltage-gated potassium channel gene. *J. Biol. Chem.* **271**, 15629-15634. doi:10.1074/jbc.271.26.15629

Xu, H., Guo, W. and Nerbonne, J. M. (1999). Four kinetically distinct depolarization-activated K+ currents in adult mouse ventricular myocytes. *J. Gen. Physiol.* **113**, 661-678. doi:10.1085/jgp.113.5.661

Xu, L., Pan, L., Li, J., Huang, B., Feng, J., Li, C., Wang, S., The, E., Liu, Y., Yuan, T. et al. (2015). Nucleoporin 35 regulates cardiomyocyte pH homeostasis by controlling Na^+-H^+ exchanger-1 expression. *J. Mol. Cell Biol.* **7**, 476-485. doi:10.1093/jmcb/mjv054

Zarayskiy, V. V., Balasubramanian, G., Bondarenko, V. E. and Morales, M. J. (2005). Heteropoda toxin 2 is a gating modifier toxin specific for voltage-gated K+ channels of the Kv4 family. *Toxicon* **45**, 431-442. doi:10.1016/j.toxicon.2004.11.015

Zhang, X., Chen, S., Yoo, S., Chakrabarti, S., Zhang, T., Ke, T., Oberti, C., Yong, S. L., Fang, F., Li, L. et al. (2008). Mutation in nuclear pore component NUP155 leads to atrial fibrillation and early sudden cardiac death. *Cell* **135**, 1017-1027. doi:10.1016/j.cell.2008.10.022